MITSUBISHI ELECTRIC RESEARCH LABORATORIES
http://www.merl.com

Lyapunov-Based Control of the Sway Dynamics for Elevator Ropes

Benosman, M.; Fukui, D.

TR2014-067 June 2014

Abstract

In this work we study the problem of rope sway dynamics control for elevator systems. We formulate this problem as a bilinear control problem and propose nonlinear controllers based on Lyapunov theory, to stabilize the rope sway dynamics. We study the stability of the proposed controllers, and test their performances on a numerical example.

American Control Conference (ACC), 2014

Lyapunov-Based Control of the Sway Dynamics for Elevator Ropes

Mouhacine Benosman and Daiki Fukui

***Abstract*— In this work we study the problem of rope sway dynamics control for elevator systems. We formulate this problem as a bilinear control problem and propose nonlinear controllers based on Lyapunov theory, to stabilize the rope sway dynamics. We study the stability of the proposed controllers, and test their performances on a numerical example.**

I. Introduction

The growing demand for high-rise buildings motivates the problem of rope sway control, which is very important in order to maintain a high safety level of the elevator system. Indeed, even slight external disturbances on the building, e.g. wind gust or earthquake, at such dimensions of structures can lead to important rope sway within the elevator shaft. Considering the length of the ropes and their heavy weight, it is clear that the rope sway can damage the equipments that are installed in the elevator shaft and can also cause damages to the elevator shaft structure itself, without mentioning the potential danger caused for the elevator passengers. For these reasons, it is very important to be able to control the rope dynamics within the elevator shaft. Furthermore, due to cost constraints, it is preferable to be able to do so, with minimum actuation capabilities. Many papers have been dedicated to the problem of modelling and control of long elevator ropes [1], [2], [3], [4], [5], [6]. In [6], a simple model of a cable attached to an actuator at its free end is used to investigate the stiffening effect of the control force on the cable. An energy analysis is used to tune an open-loop sinusoidal force applied to the cable. In [4], a scaled model for high-rise, high-speed elevators is developed. The model is used to analyze the influence of the car motion profiles on the lateral vibrations of the elevator cables. An active stiffness control of the transverse vibrations of elevator ropes is presented in [1]. The author propose a nonlinear modal feedback to drive an actuator pulling on one end of the rope. The control performance is investigated by numerical tests. In [5], the authors proposed a novel idea to dissipate the transversal energy of an elevator rope. The authors used a passive damper attached between the car and the rope. Numerical analysis of the transverse motion average energy was conducted to find the optimal value of the damper coefficient.

In this work we propose to investigate the problem of elevators' rope sway mitigation as a nonlinear control problem. Following [1], we use an active actuator to pull on one-side of the ropes. We show that in this case the model of the elevator rope together with its actuator writes as a bilinear model (in the control theory sense), and we use this bilinear model to develop nonlinear Lyapunov-based feedback controllers to stabilize the rope sway dynamics. We study the stability of the closed-loop dynamics, and show the performances of these controllers on a numerical example.

The paper is organized as follows: We start the paper with some preliminaries in Section II. In Section III, we recall the model of the system and underline its state-control bilinear form. Next, in Section IV, we present the main results of this work, namely, the nonlinear Lyapunov-based controllers, together with their stability analysis. Section V is dedicated to some numerical results. Finally, we conclude the paper with a brief summary of the results in Section VI.

II. Notations and preliminaries

Throughout the paper, $\mathbb{R}$, $\mathbb{R}_+$ denotes the set of real, and the set of nonnegative real numbers, respectively. For $x \in \mathbb{R}^N$ we define $|x| = \sqrt{x^T x}$, we denote by $A_{ij},\ i = 1, ..., n,\ j = 1, ..., m$ the elements of the matrix A, and denote by $sgn(.)$ the signum function.

III. Elevator Rope Modelling

In this section we first introduce the infinite dimension model, i.e partial differential equation (PDE), of a moving hoist cable, with non-homogenous boundary

Mouhacine Benosman (m_benosman@ieee.org) is with Mitsubishi Electric Research Laboratories, 201 Broadway Street, Cambridge, MA 02139, USA.

Daiki Fukui (Fukui.Daiki@ah.MitsubishiElectric.co.jp) is with Advanced Technology R&D Center Mitsubishi Electric Corp, 8-1-1 Tsukaguchi Honmachi, Amagasaki City, Hyogo, JAPAN

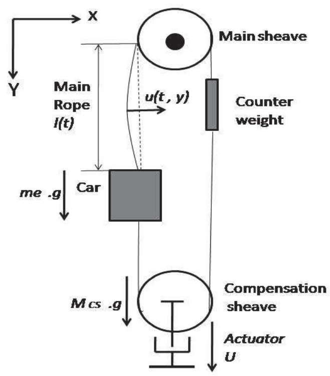

Fig. 1. Schematic representation of an elevator shaft showing the different variables used in the model

conditions. Secondly, to be able to reduce the PDE model to an ODE model using a Galerkin reduction method, we introduce a change of variables and re-write the first PDE model in a new coordinates, where the new PDE model has zero boundary conditions. Let us first enumerate the assumptions under which our model is valid.

- The elevator ropes are modelled within the framework of string theory.
- The elevator car is modelled as a point mass.
- The vibration in the second lateral direction is not included.
- The suspension of the car against its guide rails is assumed to be rigid.

Under the previous assumption, following [3], [1], the general PDE model of an elevator rope, depicted on Figure 1, is given by

$$\begin{aligned}&\rho\big(\tfrac{\partial^2}{\partial t^2}+v^2(t)\tfrac{\partial^2}{\partial y^2}+2v(t)\tfrac{\partial}{\partial y\partial t}+a\tfrac{\partial}{\partial y}\big)u(y,t)\\&-\tfrac{\partial}{\partial y}T(y,t)\tfrac{\partial u(y,t)}{\partial y}+c_p\big(\tfrac{\partial}{\partial t}+v(t)\tfrac{\partial}{\partial y}\big)u(y,t)=0\end{aligned} \tag{1}$$

where $u(y,t)$ is the lateral displacement of the rope. ρ is the mass of the rope per unit length. T is the tension in the rope, which varies depending on which rope in the elevator system we are modelling, i.e. main rope, compensation rope, etc. c_p is the damping coefficient of the rope per unit length. $v = \frac{\partial l(t)}{\partial t}$ is the elevator rope velocity, where $l: \mathbb{R} \to \mathbb{R}$ is a function (at least C^2) modelling the time-varying rope length. $a = \frac{\partial^2 l(t)}{\partial t^2}$ is the elevator rope acceleration.

The PDE (1) is associated with the following two boundary conditions:

$$\begin{aligned}u(0,t)&=f_1(t)\\u(l(t),t)&=f_2(t)\end{aligned} \tag{2}$$

where $f_1(t)$ is the time varying disturbance acting on the rope at the level of the machine room, due to external disturbances, e.g. wind gust. $f_2(t)$ is the time varying disturbance acting at the level of the car, due to external disturbances. In this work we assume that the two boundary disturbances acting on the rope are related via the relation:

$$f_2(t) = f_1(t)sin\big(\frac{\pi(H-l)}{2H}\big),\ H \in \mathbb{R} \tag{3}$$

where H is the height of the building. This expression is an approximation of the propagation of the boundary disturbance f_1 along the building structure, based on the length l, it leads to $f_2 = f_1$ for a length 0 (which is expected), and a decreasing force along the building until is vanishes at $l = H$, $f_2 = 0$ (which makes sense, since the effect of any disturbance f_1, for example wind gusts, is expected to vanish at the bottom of the building). As we mentioned earlier the tension of the rope $T(y)$ depends on the type of the rope that we are dealing with. In the sequel, we concentrate on the main rope of the elevator, the remaining ropes are modelled using the same steps by simply changing the rope tension expression.

For the case of the main rope, the tension is given by

$$T(y,t) = (m_e+\rho(l(t)-y))(g-a(t))+0.5M_{cs}g+U(t) \tag{4}$$

where g is the standard gravity constant, m_e, M_{cs} are the mass of the car and the compensating sheave, respectively, and $U(t)$ is the control tension applied by an actuator attached to the compensation sheave (the same actuator placement has been considered in [1]).

Next, we reduce the PDE model (1) to a more tractable model for control, using a projection Galerkin method or assumed mode approach, e.g. [7], [8].

To be able to apply the assumed mode approach, let us first apply the following one-to-one change of coordinates[1] to the equation (1)

$$u(y,t) = w(y,t) + \frac{l(t)-y}{l(t)}f_1(t) + \frac{y}{l(t)}f_2(t) \tag{5}$$

One can easily see that this change of coordinates implies trivial boundary conditions

$$\begin{aligned}w(0,t)&=0\\w(l(t),t)&=0\end{aligned} \tag{6}$$

[1]This change of coordinates is needed to write to original PDE model as an equivalent PDE with homogenous boundary conditions. To the best of our knowledge, it has not been proposed in previous work on elevator ropes modelling, and is newly introduced in this paper.

After some algebraic and integral manipulations, the PDE model (1) writes in the new coordinates as

$$\begin{array}{l}\rho\frac{\partial^2 w}{\partial t^2}+2v(t)\rho\frac{\partial^2 w}{\partial y\partial t}+\left(\rho v^2-T(y,t)\right)\frac{\partial^2 w}{\partial y^2}+G(t)\frac{\partial w}{\partial y}\\ +c_p\frac{\partial w}{\partial t}=y\left(-\rho s_1(t)-c_p s_2(t)\right)-\rho f_1^{(2)}+s_4(t)\end{array} \tag{7}$$

where $G(t)=\rho a(t)-\frac{\partial T}{\partial y}+c_p v(t)$, and the s_i variables are defined as

$$\begin{array}{l}s_1(t)=\frac{l l^{(2)}-2\dot{l}^2}{l^3}f_1(t)+2\frac{\dot{l}}{l^2}\dot{f}_1\\ +\frac{(l^3 f_2^{(2)}-f_2 l^2 l^{(2)}+2l\dot{l}^2 f_2-2l^2\dot{l}\dot{f}_2)}{l^4}-\frac{f_1^{(2)}}{l}\\ s_2(t)=\frac{\dot{l}}{l^2}f_1-\frac{\dot{f}_1}{l}+\frac{\dot{f}_2}{l}-f_2\frac{\dot{l}}{l^2}\\ s_3(t)=\frac{f_2-f_1}{l}\\ s_4(t)=-2v(t)\rho s_2(t)-G(t)s_3(t)-c_p\dot{f}_1(t)\end{array} \tag{8}$$

associated with the two-point boundary conditions

$$w(0,t)=0,\ \ w(l(t),t)=0. \tag{9}$$

Now instead of dealing with the PDE (1) with non-zero boundary conditions, we can use the equivalent model, given by equation (7) associated with trivial boundary conditions (9).

Following the assumed-modes technique, the solution of the equation (7), (9) writes as

$$w(y,t)=\sum_{j=1}^{j=N}q_j(t)\phi_j(y,t),\ \ N\in\mathbb{N} \tag{10}$$

where N is the number of bases (modes), included in the discretization, $\phi_j,\ j=1,...,N$ are the discretization bases and $q_j,\ \ j=1,..,N$ are the discretization coordinates. In order to simplify the analytic manipulation of the equations, the base functions are chosen to satisfy the following normalization constraints

$$\int_0^{l(t)}\phi_j^2(y,t)dy=1,\ \int_0^{l(t)}\phi_i(y,t)\phi_j(y,t)dy=0,\ \ \forall i\neq j \tag{11}$$

To further simplify the base functions, we define the normalized variable, e.g. [5], [3]

$$\xi(t)=\frac{y(t)}{l(t)} \tag{12}$$

and the normalized base functions

$$\phi_j(y,t)=\frac{\psi_j(\xi)}{\sqrt{l(t)}},\ \ j=1,...,N \tag{13}$$

In these new coordinates the normalization constraints (11) write as

$$\int_0^1\psi_j^2(\xi)d\xi=1,\ \int_0^1\psi_i(\xi)\psi_j(\xi)d\xi=0,\ \ \forall i\neq j \tag{14}$$

After classical (e.g. refer to [3]) discretization of the PDE-based model (7), (9), we can write the reduced ODE-model based on N-modes as

$$M\ddot{q}+C\dot{q}+(K+\beta U)q=F(t),\ q\in\mathbb{R}^N,\ F\in\mathbb{R}^N \tag{15}$$

where

$$\begin{array}{l}M_{ij}=\rho\delta_{ij}\\ C_{ij}=\rho l^{-1}\dot{l}\left(2\int_0^1(1-\xi)\psi_i(\xi)\psi_j'(\xi)d\xi-\delta_{ij}\right)+c_p\delta_{ij}\\ K_{ij}=\frac{1}{4}\rho l^{-2}\dot{l}^2\delta_{ij}-\rho l^{-2}\dot{l}^2\int_0^1(1-\xi)^2\psi_i'(\xi)\psi_j'(\xi)d\xi\\ +\rho l^{-1}(g-a(t))\int_0^1(1-\xi)\psi_i'(\xi)\psi_j'(\xi)d\xi+m_e l^{-2}(g-a(t))\int_0^1\psi_i'(\xi)\psi_j'(\xi)d\xi\\ +\rho(l^{-2}\dot{l}^2-l^{-1}\ddot{l})\left(0.5\delta_{ij}-\int_0^1(1-\xi)\psi_i(\xi)\psi_j'(\xi)d\xi\right)-\\ c_p\dot{l}l^{-1}(\int_0^1\psi_i(\xi)\psi_j'(\xi)\xi d\xi+0.5\delta_{ij})+0.5M_{cs}gl^{-2}\int_0^1\psi_i'(\xi)\psi_j'(\xi)d\xi\\ +U(t)l^{-2}\int_0^1\psi_i'(\xi)\psi_j'(\xi)d\xi\\ \beta_{ii}=l^{-2}\int_0^1\psi_i'^2 d\xi=l^{-2}\tilde{\beta}_{ii}\\ \beta_{ij}=\tilde{\beta}_{ij}=0,\ \forall\ i\neq j\\ F_i(t)=-l\sqrt{l}(\rho s_1(t)+c_p s_2(t))\int_0^1\psi_i(\xi)\xi d\xi\\ +\sqrt{l}\left(s_4(t)-\rho f_1^{(2)}(t)\right)\int_0^1\psi_i(\xi)d\xi\\ \delta_{ij}=\begin{cases}0,\ i\neq j\\ 1,\ i=j\end{cases}\end{array} \tag{16}$$

where $s_i,\ i=1,2,3,4$ are given in (8).

Remark 1: 1- In the previous developments we have neglected the bending stiffness of the rope, introducing it back does not change the obtained models. Indeed, if we consider that the rope material and shape implies a bending stiffness coefficient EI (where E is the material Young modulus and I is moment of inertia of the cross section of the rope), the model equation (15) remains valid (e.g. [3]) with the addition of the following term in the stiffness matrix K

$$\tilde{K}_{ij}=EIl^{-4}\int_0^1\psi_i^{(2)}(\xi)\psi_j^{(2)}(\xi)d\xi \tag{17}$$

we see that these new terms are inversely proportional to l^4, which makes them negligible for long ropes, furthermore, their addition does not change the structure of the model and thus does not alter the results of this paper.

2- The model (15), (16) has been obtained for the general case of time-varying rope length $l(t)$, however, in this paper we only consider the case of stationary ropes $l=cte$, which is directly deduced from (15), (16), by setting $\dot{l}=\ddot{l}=0,\ \forall t$.

If we use the classical definition of the state vector $z=(q,\dot{q})^T$, then it is easy to see that the obtained ODE model is a bilinear model in the state z and the control vector U.

IV. Main result: Lyapunov-based controllers

In this section we present Lyapunov-based feedback controllers designed to stabilize the rope sway dynamics.

Theorem 1: Consider the rope dynamics (15), (16), with non-zero initial conditions, with no external disturbances, i.e. $f_1(t) = f_2(t) = 0, \forall t$, and with constant length l, then the feedback control

$$U_{nom-1}(z) = \begin{cases} u_{max}\frac{\dot{q}^T\tilde{\beta}q}{\sqrt{1+(\dot{q}^T\tilde{\beta}q)^2}},\ if\ \dot{q}^T\tilde{\beta}q > 0 \\ 0,\ if\ \dot{q}^T\tilde{\beta}q \leq 0 \end{cases} \tag{18}$$

where $z = (q^T, \dot{q}^T)^T$, renders the closed-loop equilibrium point $(0, 0)$ globally asymptotically stable, with $|U_{nom-1}| \leq u_{max}$, furthermore $|U_{nom-1}|$ decreases as function of $\dot{q}^T\tilde{\beta}q$.

Proof: We define the control Lyapunov function as

$$V(z) = \frac{1}{2}\dot{q}^T(t)M\dot{q}(t) + \frac{1}{2}q^T(t)Kq(t) \tag{19}$$

where $x = (q^T, \dot{q}^T)^T$.
First we compute the derivative of the Lyapunov function along the dynamics (15), without disturbances, i.e. $F(t) = 0,\ \forall t$

$$\begin{aligned} \dot{V}(z) &= \dot{q}^T(-C\dot{q} - Kq - \beta Uq) + q^TK\dot{q} \\ &= -\dot{q}^TC\dot{q} - \dot{q}^T\beta qU \end{aligned} \tag{20}$$

To ensure the negative definiteness of $\dot{V}(x)$ we define the first controller (18). Using the continuity of (18) at $\dot{q}^T\tilde{\beta}q = 0$ and LaSalle theorem, e.g. [9], we can conclude that the states of the closed-loop dynamics converge to the set $S = \{z = (q^T, \dot{q}^T)^T \in \mathbb{R}^{2N},\ s.t.\ \dot{q} = 0\ \}$. Next, we analyze the closed-loop dynamics: Since the boundedness of V implies boundedness of $\dot{q},\ q$ and by equation (15), boundedness of $\ddot{q}$. Boundedness of $\dot{q},\ \ddot{q}$ implies the uniform continuity of $q,\ \dot{q}$, which again by (15), implies the uniform continuity of $\ddot{q}$. Next, since $\dot{q} \to 0$, and using Barbalat's Lemma, e.g. [9], we conclude that $\ddot{q} \to 0$, and by invertibility of the stiffness matrix $K + \beta U$ we conclude that $q \to 0$. Finally, the fact that V is a radially unbounded function, ensures that the equilibrium point $(q, \dot{q}) = (0, 0)$ is globally asymptotically stable. Furthermore the fact that $|U_{nom-1}| \leq u_{max}$, and the decrease of $|U_{nom-1}|$ as function of $\dot{q}^T\tilde{\beta}q$ is deduced from equation (18). ■

Remark 2: By examining the Lyapunov derivative (20), we can see that instead of the C^0 controller (18), we could use a smooth controller of the form

$$U_{nom-1}(z) = u_{max}\frac{\dot{q}^T\tilde{\beta}q}{\sqrt{1 + (\dot{q}^T\tilde{\beta}q)^2}}$$

However, the advantage of the switching controller (18) is the fact that it necessitates less control energy, since when the condition $\dot{q}^T\tilde{\beta}q \leq 0$ is satisfied, it does not apply any extra control and only uses the system's natural damping.

The nominal controller U_{nom-1} given by (18) does not take into account the disturbance $F(t)$ explicitly. We present next a controller that takes into account $F(t)$ in the design of the control law. However, since in practical applications we seldom have access to direct measurements of the disturbance signal $F(t)$, we use the so called Lyapunov reconstruction technique, e.g. [10], to augment the nominal controller U_{nom-1} with an additional feedback term which is based only on an upper bound of the disturbance signal $F(t)$ (i.e. does not need the exact measurements of $F(t)$) and which ensures the stabilization of the sway to a small amplitude, which can be tuned by the choice of the feedback gains.

First let us state the following assumption.

Assumption 1: The time varying disturbance functions $f_1,\ f_2$ are such that, the function $F(t)$ is bounded, i.e. $\exists F_{max},\ s.t.\ |F(t)| \leq F_{max},\ \forall t$.

Theorem 2: Consider the rope dynamics (15), (16), under non-zero external disturbances, i.e. $f_1(t) \neq 0,\ f_2(t) \neq 0$, and with constant length l, then under Assumption 1, the feedback control

$$\begin{aligned} &U(z) = U_{nom-1}(z) + ksgn(\dot{q}^T\tilde{\beta}q)(F_{max} + \epsilon)|\dot{q}|, \\ &\ k > 0, \epsilon > 0 \end{aligned} \tag{21}$$

where $z = (q^T, \dot{q}^T)^T$, ensures that the solutions of (15), (16) and (21) converges to the invariant set $\tilde{S} = \{(q^T, \dot{q}^T)^T \in \mathbb{R}^{2N},\ s.t.\ kl^{-2}|\dot{q}^T\tilde{\beta}q| \leq 1\ \}$.

Proof: Using the same Lyapunov function (19), and writing its derivative along (15)

$$\dot{V}(z) = -\dot{q}^TCq - \dot{q}^T\beta qU(x) + \dot{q}^TF(t) \tag{22}$$

if we denote $U(z) = U_{nom-1}(z) + v(z)$, where $v(z) = ksgn(\dot{q}^T\tilde{\beta}q)(F_{max} + \epsilon)|\dot{q}|,\ k > 0,\ \epsilon > 0$, we obtain

$$\begin{aligned} \dot{V}(z) = -\dot{q}^TCq - \dot{q}^T\beta qU_{nom-1}(x) - \dot{q}^T\beta qv(x) \\ +\dot{q}^TF(t) \end{aligned} \tag{23}$$

and by definition of $U_{nom-1}(z)$ we know that

$$-\dot{q}^T C q - \dot{q}^T \beta q U_{nom-1}(z) < 0$$

thus, using Assumption 1, we can write

$$\begin{aligned}
&\dot{V}(z) \leq -\dot{q}^T \beta q v(z) + \dot{q}^T F(t) \\
&\leq -kl^{-2}|\dot{q}^T \tilde{\beta} q|(F_{max} + \epsilon)|\dot{q}| + |\dot{q}||F(t)| \\
&\leq -kl^{-2}|\dot{q}^T \tilde{\beta} q|(F_{max} + \epsilon)|\dot{q}| + |\dot{q}|F_{max} \\
&\leq -kl^{-2}|\dot{q}^T \tilde{\beta} q||\dot{q}|\epsilon + |\dot{q}|F_{max}(1 - kl^{-2}|\dot{q}^T \tilde{\beta} q|) \\
&\leq +|\dot{q}|F_{max}(1 - kl^{-2}|\dot{q}^T \tilde{\beta} q|)
\end{aligned}$$

which proves the decrease of $V(x)$ until reaching the invariant set

$$\tilde{S} = \{(q^T, \dot{q}^T)^T \in \mathbb{R}^{2N},\ s.t.\ kl^{-2}|\dot{q}^T \tilde{\beta} q| \leq 1\ \}$$

■

Remark 3: The controllers (18), (21) are state feedbacks based on q, $\dot{q}$, these states can be easily computed from the sway measurements at N given positions $y(1), ..., y(N)$, via equation (10). The sway $w(y,t)$ can be measured by laser displacement sensors placed at the positions $y(i)$, $i = 1, 2, ...N$, along the rope, e.g.[11], subsequently q can be computed by simple algebraic inversion of (10), and $\dot{q}$ can be obtained by direct numerical differentiation of q.

Remark 4: The controller (21) has a discontinuity due to the sgn function. For practical implementation, well known regularization can be used to smoothen the controller, for example a sat function can be used instead of the sgn function, and similar stability results can be concluded (e.g. refer to [10]). Due to space limitation, we do not present the regularized version of the controller here, and defer it to a longer journal version of this work.

V. NUMERICAL EXAMPLE

In this section we present some numerical results obtained on the example presented in [1]. The case of an elevator system with the mechanical parameters summarized on Table I has been considered for the tests presented hereafter. We write the controllers based on the model (15), (16) with one mode, but we test them a model with three modes (the fact is that one mode is enough since when comparing the solution of the PDE (7) to the discrete model (15) the higher modes shown to be negligible, and a discrete model with one mode showed a very good match with the PDE model, but to make the simulation tests more realistic we chose to test the controllers on a three modes model[2]). First, to validate Theorem 1, we present the results obtained by applying the controller (18), to the model (15), (16), with non-zero initial conditions $q(0) = 20$, $\dot{q}(0) = 0$, and zero external disturbances, i.e. $f_1(t) = f_2(t) = 0,\ \forall t$. In these first tests, to show the effect of the controller (18) alone, without the 'help' of the system's natural damping, we fix the damping coefficient to zero, i.e. $c_p = 0$. Figures 2, 3[3] show the rope sway obtained at half rope-length $y = 195\ m$ without control. It reaches a maximum value of about $1.45\ m$. We show next on Figures 4, 5 the rope sway obtained at the same rope length but this time with the controller (18), with $u_{max} = 1500\ N$. We see the expected effect of the controller on the sway, which is reduced by half in about 60 sec and vanishes asymptotically. The corresponding control force is depicted on Figures 6, 7. We see that, as expected from the theoretical analysis of Theorem 1, the control force remains bounded by u_{max} and decreases with the decrease of the sway.

Parameters	**Definitions**	**Values**
n	Number of ropes	$8[-]$
m_e	Mass of the car	$3500[kg]$
ρ	Main rope linear mass density	$2.11[kg/m]$
l	Rope maximum length	$390[m]$
H	Building height	$402.8[m]$
c_p	Damping coefficient	$0.0315[N.sec/m]$

TABLE I

NUMERICAL VALUES OF THE MECHANICAL PARAMETERS

Next, we consider the model (15), (16) with nozero disturbance signals: $f_1(t) = 0.2sin(2\pi.0.08t)$, and f_2 being deduced from f_1 via equation (3). We underline that we have purposely selected the disturbance frequency to be equal to the first resonance frequency of the rope, to simulate the 'worst-case scenario'. We first show on Figures 8, 9 the sway signal in the uncontrolled case. Let us consider now the controller (21) introduced in Theorem 2. We apply (21), with the parameters $u_{max} = 1500\ N, F_{max} = 1.6\ , \epsilon = 0.1\ , k = 10^6$. The effect of the control on the rope sway amplitude is depicted on Figures 10, 11. The rope sway is effectively reduced, and enters

[2]We also want to inform the reviewers that these controllers have been actually validated on a full-size test-bed in Japan, unfortunately, due to IP reasons we were not allowed to report the experimental data here (This footnote is added for the reviewers but will be deleted in the final version of the paper).

[3]The figures' zoom is included for the reader to have a better idea about the signals shape.

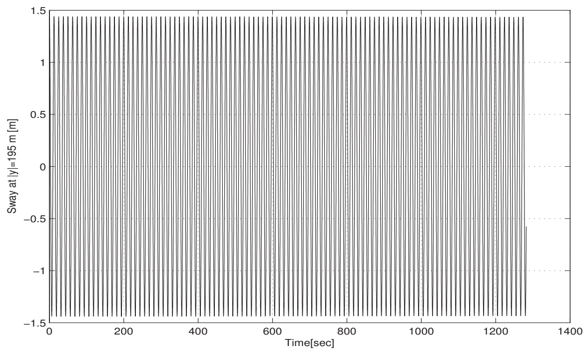

Fig. 2. Rope sway at $y = 195$ m- No control with zero disturbance

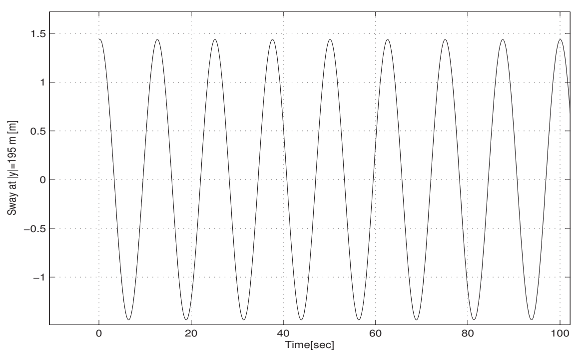

Fig. 3. Zoom of the rope sway at $y = 195$ m- No control with zero disturbance

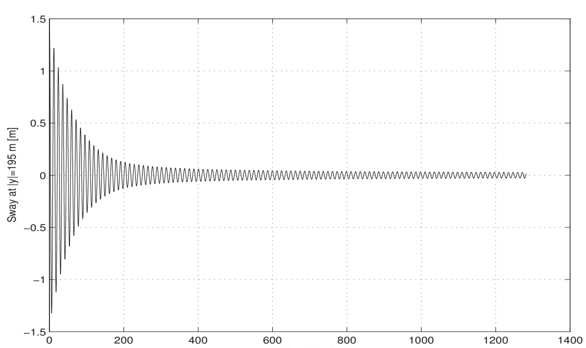

Fig. 4. Rope sway at $y = 195$ m- with controller (18)

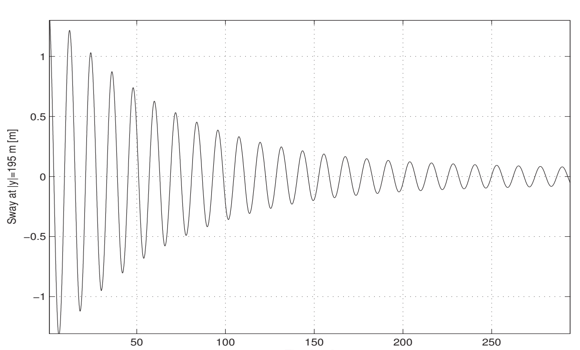

Fig. 5. Zoom of the rope sway at $y = 195$ m- with controller (18)

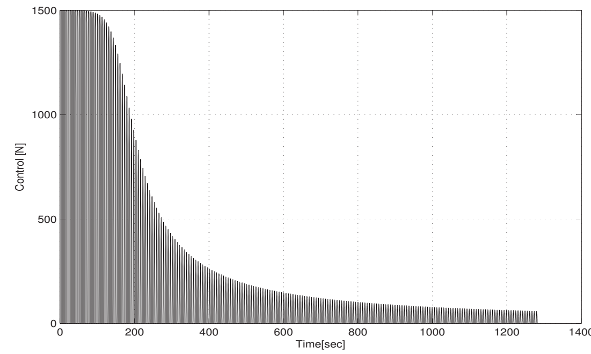

Fig. 6. Output of controller (18)

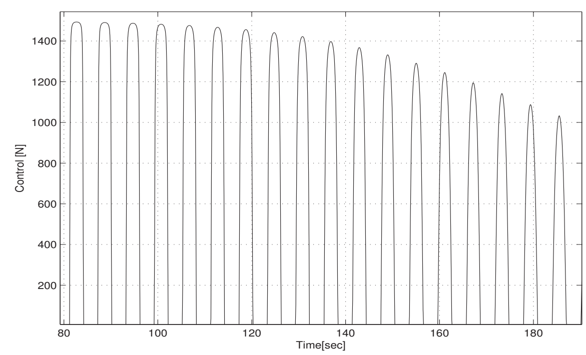

Fig. 7. Zoom of the output of controller (18)

the invariant set defined by the upper bound condition $kl^{-2}|\dot{q}\tilde{\beta}q| \leq 1$, as indicated in Theorem 2. In fact, by checking the $q\dot{q}$ plot presented on Figures 12, 13, we see that the Lagrangian variables $q, \dot{q}$ converge to the point satisfying $kl^{-2}|\dot{q}\tilde{\beta}q|_{max} = 0.97$, which is in concordance with the invariant set convergence result of Theorem 2. The control force is depicted on Figures 14, 15, which shows a high amplitude, due to the selected high gain value for k.

VI. Conclusion

In this paper we have studied the problem of active control of elevator rope sway dynamics occurring due to external force disturbances acting on the elevator system. We have considered the case of constant rope length and have proposed nonlinear controllers based on Lyapunov theory. We have presented the stability analysis of these controllers and shown their efficiency on a numerical example. The stabilization problems related to time-varying rope lengths, i.e. moving car, will be presented in a longer journal version of this work.

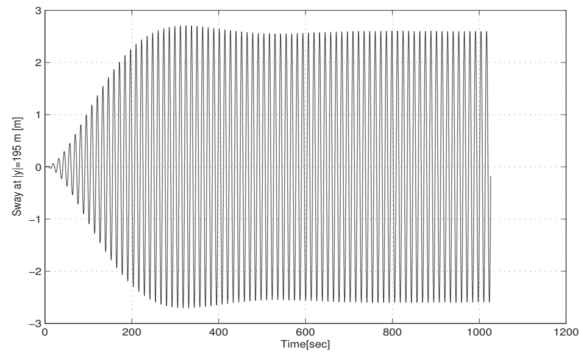

Fig. 8. Rope sway at $y = 195$ m- No control with non-zero disturbance

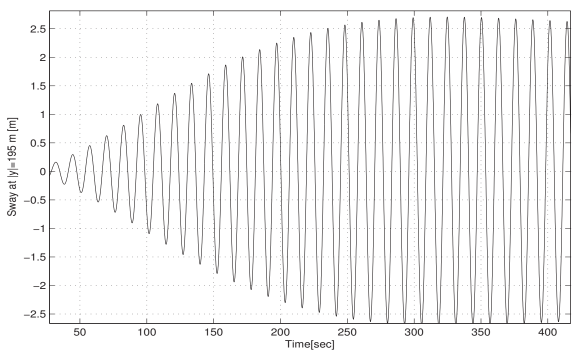

Fig. 9. Rope sway at $y = 195$ m- No control with non-zero disturbance

REFERENCES

[1] S. Kaczmarczyk, "Nonlinear sway and active stiffness control of long moving ropes in high-rise vertical transporation systems," in *The 10th International Conference on Vibration Problems*, S. P. in Physics, Ed., 2011, pp. 183–188.

[2] S. Kaczmarczyk, R. Iwankiewicz, and Y. Terumichi, "The dynamic behavior of a non-stationary elevator compensating rope system under harmonic and stochastic excitations," in *Journal of Physics: Conference Series 181*. IOP Publishing, 2009, pp. 1–8.

[3] W.D.Zhu and G. Xu, "Vibration of elevator cables with small bending stiffness," *Journal of Sound and Vibration*, vol. 263, pp. 679–699, 2003.

[4] W.D.Zhu and L. Teppo, "Design and analysis of a scaled model of a high-rise high-speed elevator," *Journal of Sound and Vibration*, vol. 264, pp. 707–731, 2003.

[5] W.D.Zhu and Y. Chen, "Theoretical and experimental investigation of elevator cable dynamics and control," *Journal of Sound and Vibration*, vol. 128, pp. 66–78, 2006.

[6] Y. Fujino, P. Warnitchai, and B. Pacheco, "Active stiffness control of cable vibration," *ASME Journal of Applied Mechanics*, vol. 60, pp. 948–953, 1993.

[7] L. Meirovitch, *Analytical methods in vibrations*, Fred Landis ed., ser. Applied Mechanics. Collier Macmillan publishers, 1967.

[8] P. Holmes, J. LUmley, and G. Berkooz, *Turbulence, coherent*

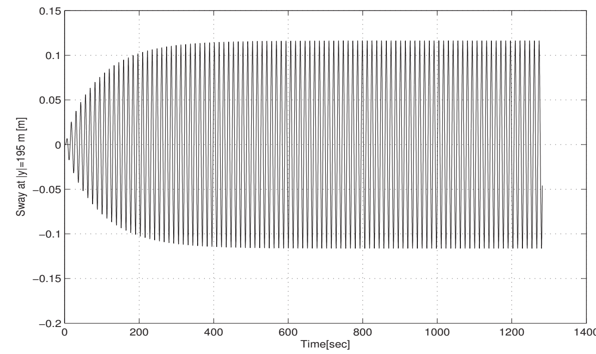

Fig. 10. Rope sway at $y = 195$ m- controller (21)

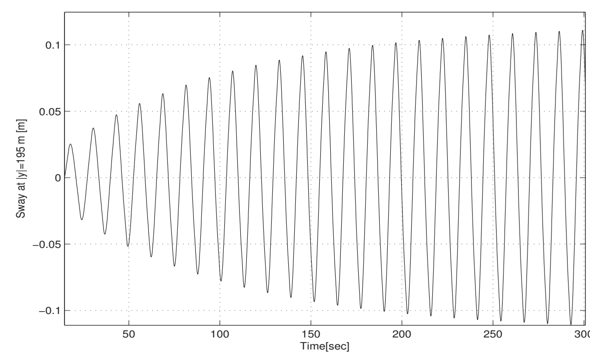

Fig. 11. Rope sway at $y = 195$ m- controller (21)

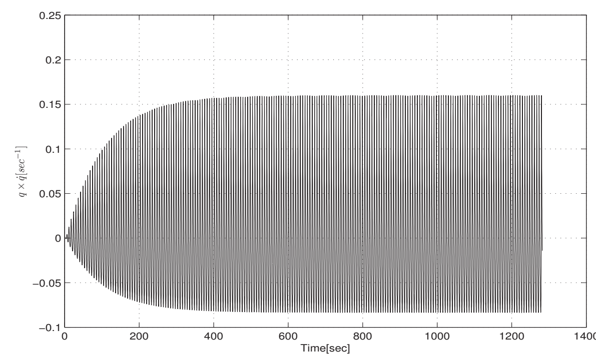

Fig. 12. $q\dot{q}$ signal- controller (21)

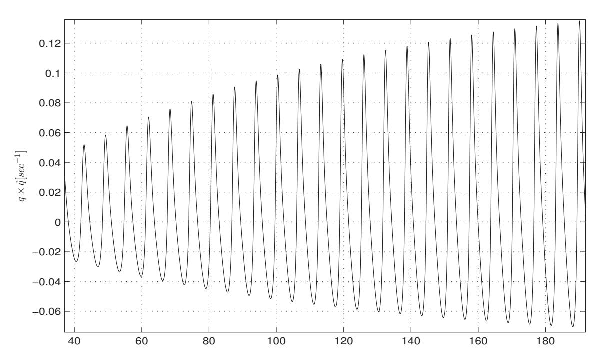

Fig. 13. $q\dot{q}$ signal- controller (21)

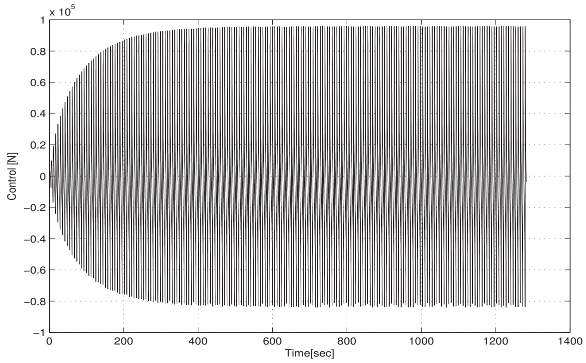

Fig. 14. Output of controller (21)

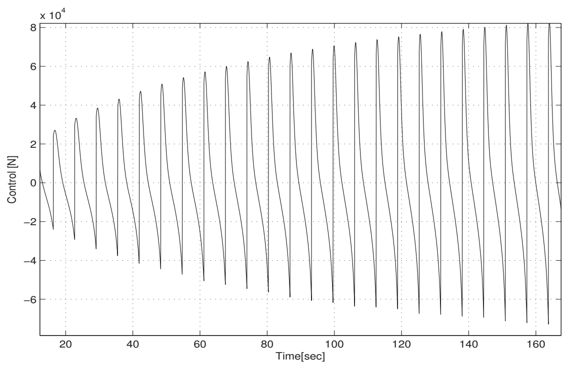

Fig. 15. Output of controller (21)

structures, dynamical systems and symmetry. UK: Cambridge University Press, 1996.

[9] H. Khalil, *Nonlinear systems*, 2nd ed. New York Macmillan, 1996.

[10] M. Benosman and K.-Y. Lum, "Passive actuators' fault tolerant control for affine nonlinear systems," *IEEE, Transactions on Control Systems Technology*, vol. 18, 2010.

[11] M. Otsuki, K. Yoshida, K. Nagata, S. Fujimoto, and T. Nakagawa, "Experimental study on vibration control for rope-sway of elevator of high-rise building," in *American Control Conference*, 2002, pp. 238–243.